

## **Supplemental Material Table of contents**

### **Supplemental Methods**

### **Supplemental Figures**

Supplemental Figure 1. The treatment effect by NMN on glucometabolism

Supplemental Figure 2. The treatment effect by NMN on metabolic changes

Supplemental Figure 3. The effect of short-term NAM treatment on HbA1c and urine ACR

Supplemental Figure 4. The effect of NMN treatment on histological changes in DN at 10 weeks of age

Supplemental Figure 5. The effect of NMN treatment on histological changes in DN at 30 weeks of age

Supplemental Figure 6. The effect of NMN treatment on profibrotic genes in glomeruli

Supplemental Figure 7. Molecular changes in glomerulus at 10 weeks of age

Supplemental Figure 8. Molecular changes in glomerulus at 30 weeks of age

Supplemental Figure 9. Effects of NMN treatment on the salvage pathway at 10 weeks of age

Supplemental Figure 10. Effects of NMN treatment on the salvage pathway at 30 weeks of age

Supplemental Figure 11. Effect of NMN treatment on acetylated p65

## **Supplemental Methods**

### **Metabolic analysis**

During and after 14 days of NMN or vehicle treatment, we evaluated metabolic parameters.

During and after treatment, the amount of food intake was examined. After treatment, IPGTT and ITT were conducted. Moreover, 15% dextrose (1.5 g/kg body weight) was injected intraperitoneally in the morning after mice were fasted for 16 h for IPGTTs. Blood was collected from the tail vein at 0, 15, 30, 60, and 120 min. Blood glucose levels were measured by the OneTouch Ultra glucometer (LifeScan Inc, Milpitas, CA, USA), and plasma insulin levels were determined using LBIS Mouse Insulin ELISA Kit (FUJIFILM Wako Shibayagi Co., Gunma, Japan). Mice were injected with insulin (0.75 U/kg body weight) in the early afternoon after being fasted for 4 h for insulin tolerance tests. Moreover, blood glucose levels were measured at 0, 15, 30, 60, and 120 min after insulin injection. Metabolic parameters including oxygen consumption, respiratory quotient (RQ;  $VO_2/VO_2$ ), and energy expenditure (EE) were measured using a mass spectrometer (Arco System, Chiba, Japan) over 24 h. Each mouse was housed per chamber with a 12-h light/12-h dark cycle at room temperature ( $22^\circ\text{C} \pm 1^\circ\text{C}$ ).

### **NAM treatment protocols**

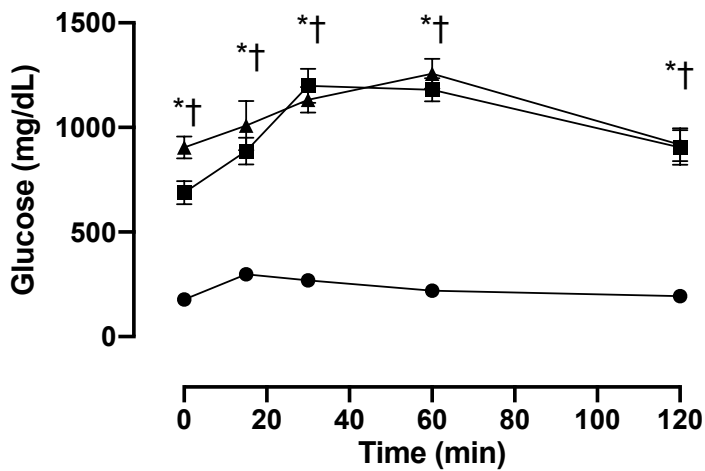
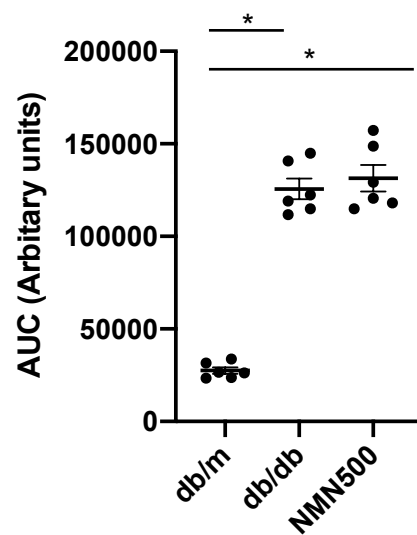
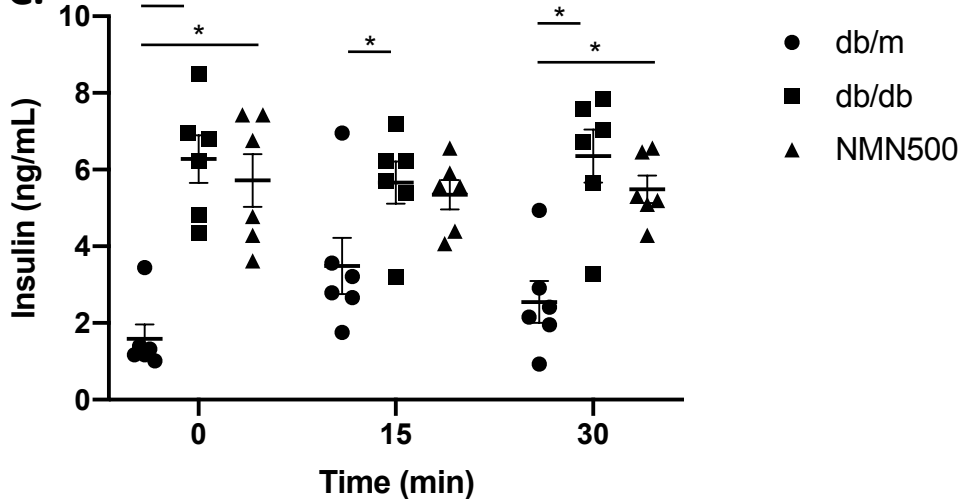
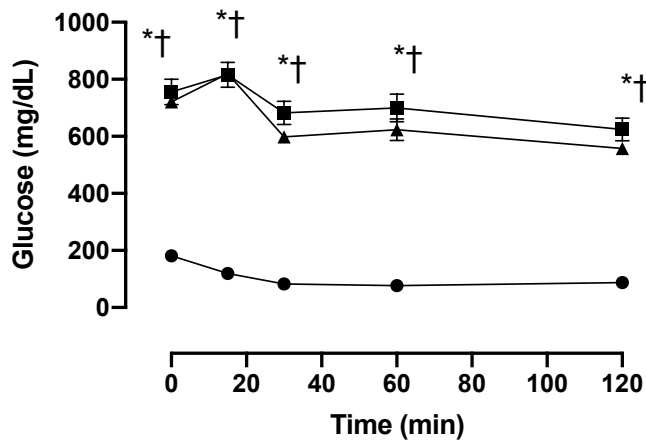
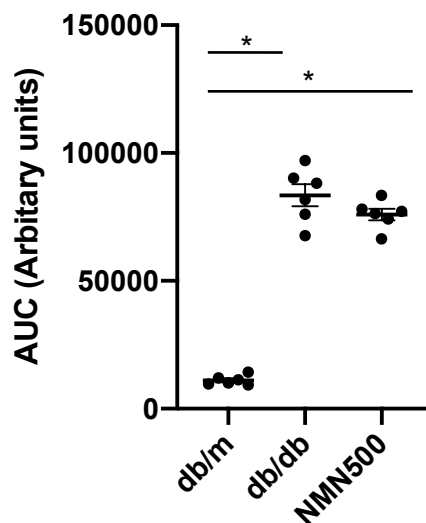
Eight-week-old male diabetic *db/db* mice (BKS.Cg-+ Leprdb/+ Leprdb/Jcl) and non-diabetic control eight-week-old male *db/m* mice (BKS.Cg-m +/+ Leprdb/Jcl) were purchased from

Japan CLEA Co. (Tokyo, Japan). The animals were housed at a constant room temperature ( $22 \pm 1$  °C) under a controlled 12-h light/12-h dark cycle. The mice had free access to water and regular chow. *Db/db* mice were randomly assigned to one of two groups: treatment with vehicle (normal saline) or treatment with NAM (200 mg/kg/day) in normal saline. *db/m* (BKS.Cg-m  $+/+$  Lepr<sup>db</sup>/Jcl) mice were treated with vehicle as non-diabetic controls. Vehicle and NAM were administered intraperitoneally every day for 14 consecutive days. HbA1c and urine analyses were performed at 10 weeks of age. All animal studies were approved by the Animal Care Committee of the Keio University School of Medicine in accordance with the national and regional guidelines.

### **Immunohistochemistry for Collagen IV and fibronectin**

IHC was performed as previously described. Briefly, paraffin sections (4  $\mu$ m) were fixed in 3% formaldehyde and stained using Collagen IV (Millipore, AB756P, 1:200) and Fibronectin (Sigma Aldrich, f3648, 1:500) primary antibodies. Goat anti-rabbit IgG (Nichirei, 414341) was used as the secondary antibody.

## Supplemental Figures

**A.****B.****C.****D.****E.**Figure S1, Yasuda *et al.*

**Figure S1. The treatment effect by NMN on glucometabolism**

(A–C) Intraperitoneal glucose tolerance test (IPGTT) at 10 weeks of age in the three groups (*db/m*, *db/db*, and NMN500; *n* = 6). Blood glucose curve in IPGTT (A). Area under the curve of IPGTT (B). Plasma insulin levels were measured at the 0, 15, and 30 min time points during the IPGTTs (C). (D and E) Insulin tolerance test (ITT) at 10 weeks of age in the three groups (*db/m*, *db/db*, and NMN500; *n* = 6). Blood glucose curve in ITT (D). Area under the curve of ITT (E). All data are shown as mean ± standard error of the mean. Statistical significance between each group is represented by a horizontal bar. \**P* < 0.05 by ANOVA with Tukey post hoc test.

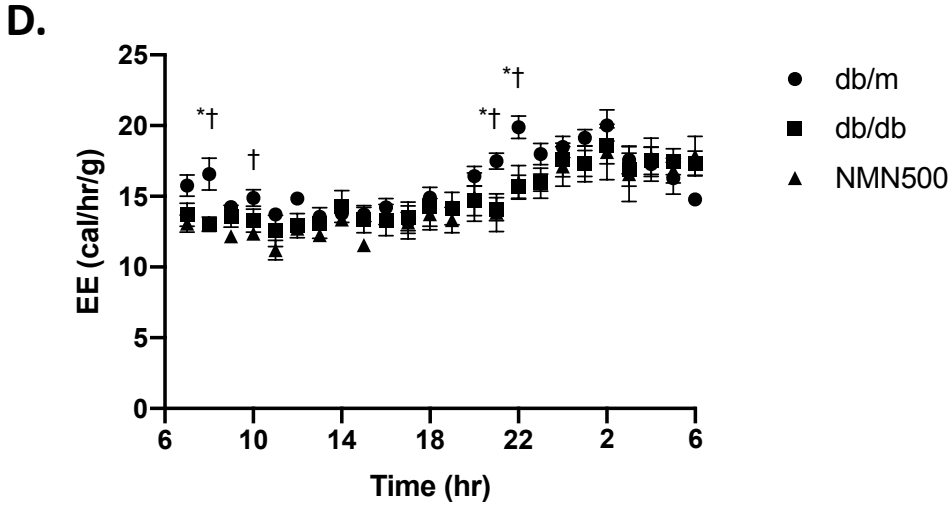
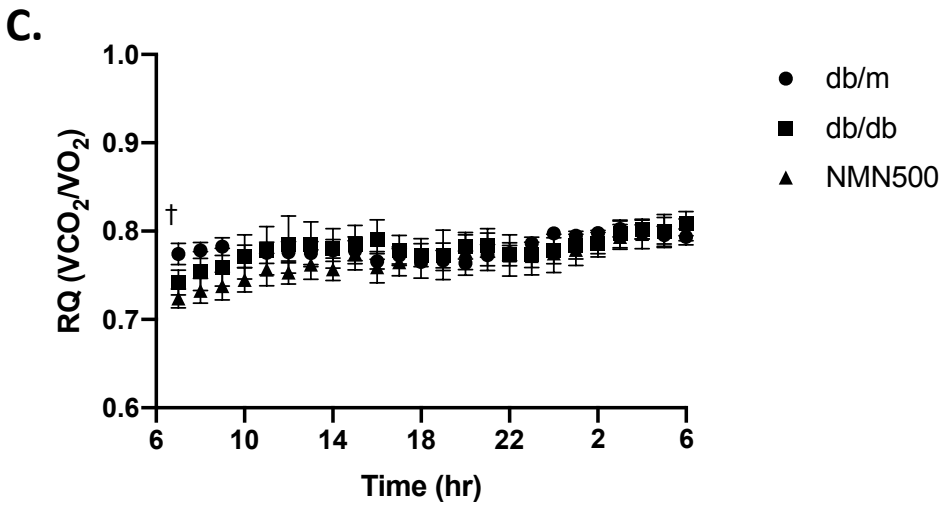
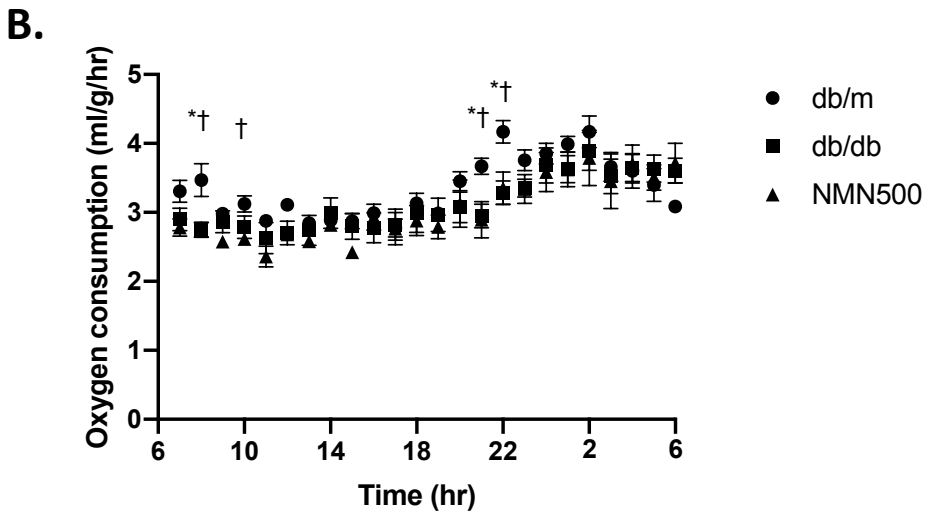
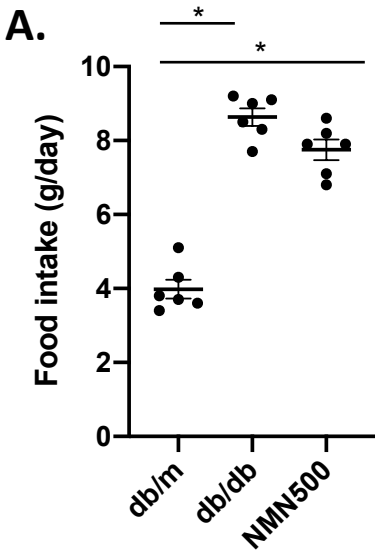
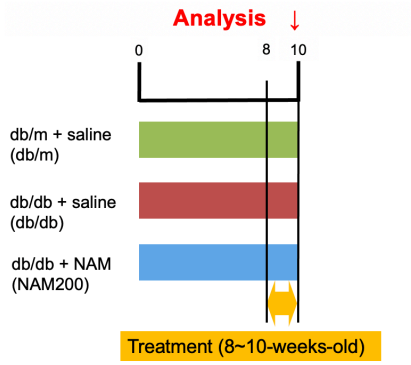
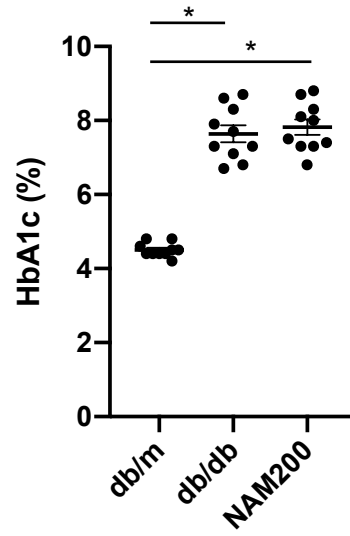
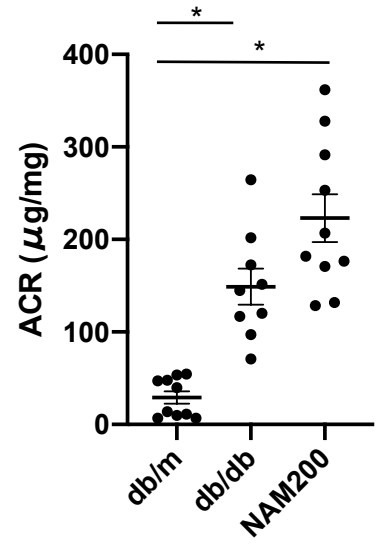


Figure S2, Yasuda *et al.*

**Figure S2. The treatment effect by NMN on metabolic changes**

(A) Food intake was measured at 10 week of age in the three groups (*db/m*, *db/db*, and NMN500;  $n = 6$ ). Statistical significance between each group is represented by a horizontal bar.  $*P < 0.05$  by ANOVA with Tukey post hoc test. (B–D) Oxygen consumption (VO<sub>2</sub>) (B), respiratory quotient (RQ) (C), and energy expenditure (EE) (D) were measured at 10 week of age using indirect calorimetry in the three groups (*db/m*, *db/db*, and NMN500;  $n = 6$ ). All data are shown as mean  $\pm$  standard error of the mean.  $*P < 0.05$  *db/m* vs. *db/db*.  $\dagger P < 0.05$  *db/m* vs. NMN500.



**A.****B.****C.**

**Figure S3. The effect of short-term NAM treatment on HbA1c and urine ACR**

(A) Schematic diagram for the nicotinamide (NAM) treatment protocol. (B) HbA1c levels at 24 weeks of age in the three groups (*db/m*, *db/db*, and NMN500; n = 10). (C) Urine ACR at 24 weeks of age in the three groups (*db/m*, *db/db*, and NMN500; n = 10). All data are shown as mean  $\pm$  standard error of the mean. Statistical significance between each group is represented by a horizontal bar. \* $P < 0.05$  by ANOVA with Tukey post hoc test.

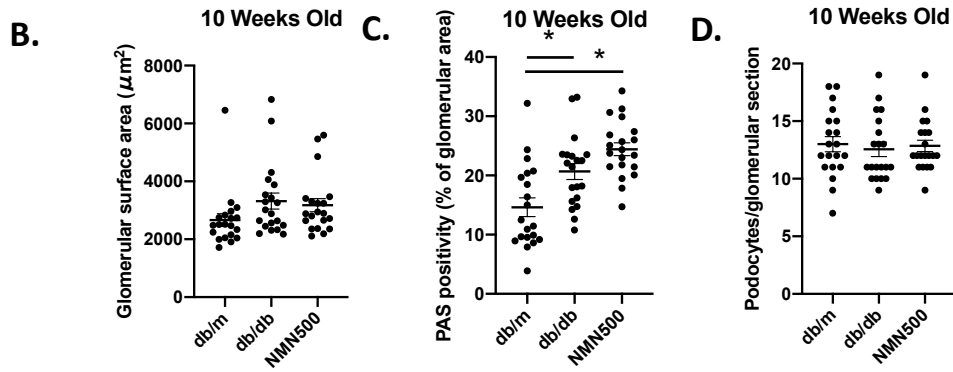
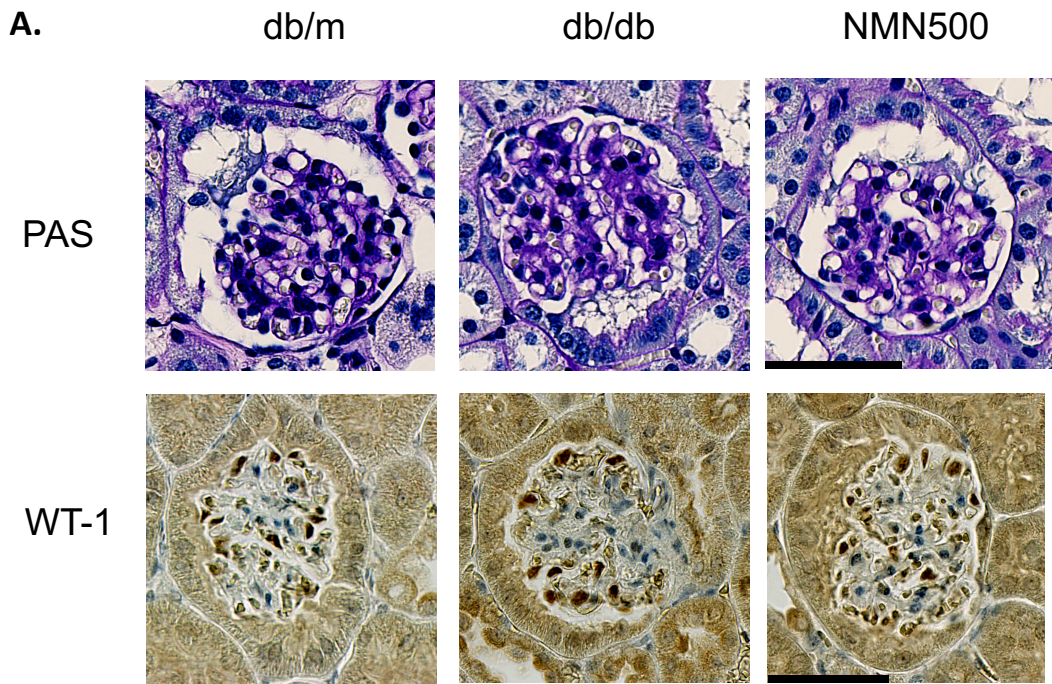


**Figure S4. The effect of NMN treatment on histological changes in DN at 10 weeks of age**

(A) Representative PAS staining and immunostaining for WT1 in the glomeruli of the *db/m*, *db/db*, and NMN500 groups at 10 weeks of age (scale bar, 50  $\mu$ m). (B, C) Glomerular surface area (B) and PAS positivity of the glomerular area (C) in PAS-stained kidney sections determined by Image-Pro Plus 7.0J software;  $n = 20$  glomerular sections per group. (D) Number of podocytes per glomerulus detected with antibodies to WT1. Podocytes/glomerular sections were determined using Image-Pro Plus 7.0J software. All data are shown as mean  $\pm$  standard error of the mean. Statistical significance between each group is represented by a horizontal bar.  $*P < 0.05$  by ANOVA with Tukey post hoc test.

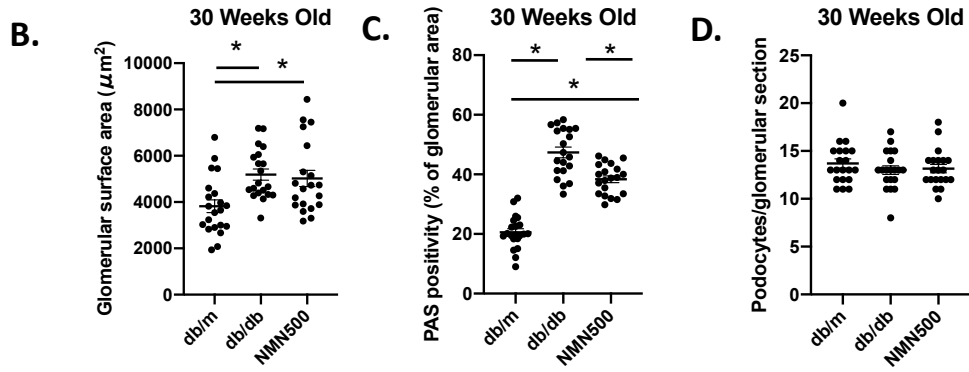
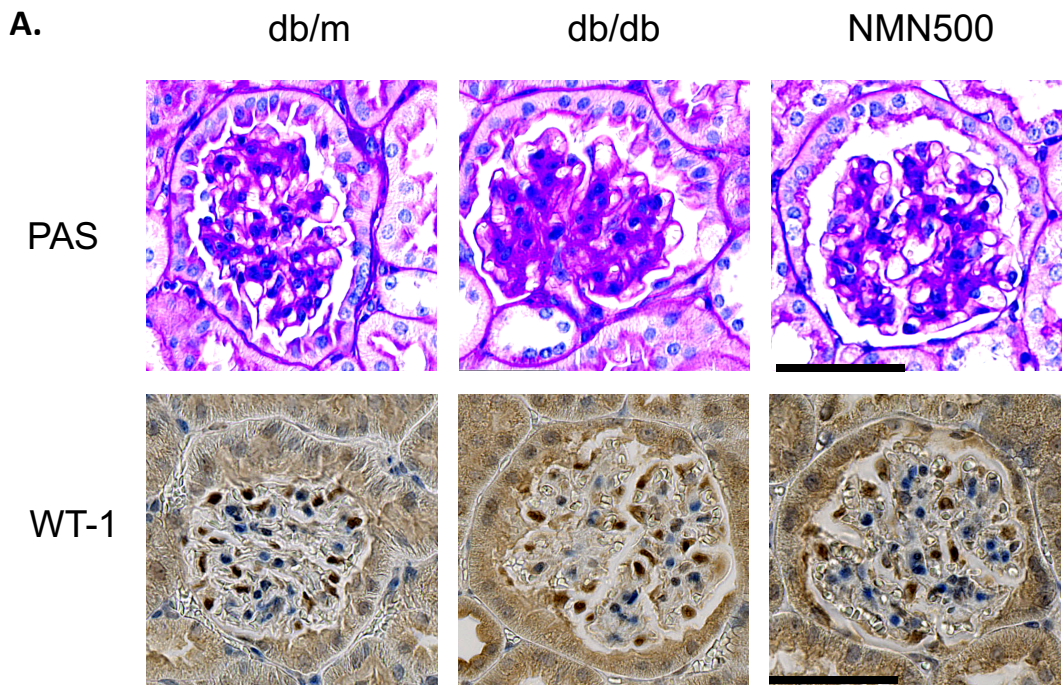


**Figure S5. The effect of NMN treatment on histological changes in DN at 30 weeks of age**

(A) Representative PAS staining and immunostaining for WT1 in the glomeruli of the *db/m*, *db/db*, and NMN500 groups at 30 weeks of age (scale bar, 50  $\mu$ m). (B, C) Glomerular surface area (B) and PAS positivity of the glomerular area (C) in PAS-stained kidney sections determined by Image-Pro Plus 7.0J software;  $n = 20$  glomerular sections per group. (D) Number of podocytes per glomerulus detected with antibodies to WT1. Podocytes/glomerular sections were determined using Image-Pro Plus 7.0J software. All data are shown as mean  $\pm$  standard error of the mean. Statistical significance between each group is represented by a horizontal bar.  $*P < 0.05$  by ANOVA with Tukey post hoc test.

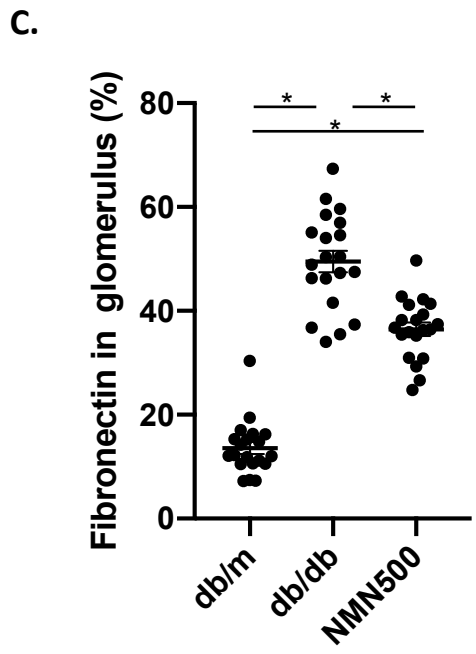
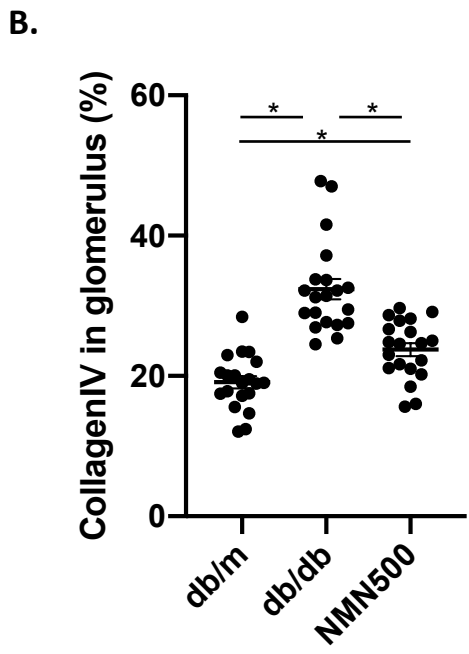
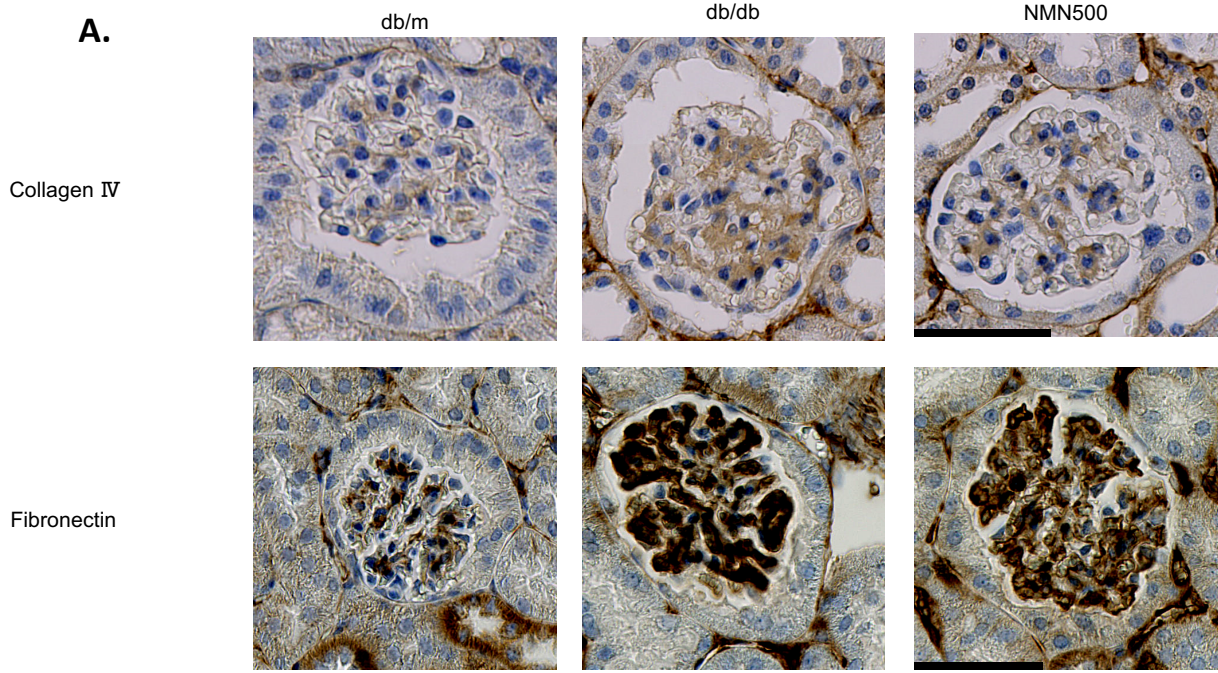


Figure S6, Yasuda *et al.*

**Figure S6. The effect of NMN treatment on profibrotic genes in glomeruli**

(A) Representative immunostaining for collagen IV and fibronectin in the glomeruli of the *db/m*, *db/db*, and NMN500 groups at 24 weeks of age (scale bar, 50  $\mu\text{m}$ ). (B, C) Proportional areas of collagen IV (B) and fibronectin (C) staining determined by Image-Pro Plus 7.0J software ( $n = 20$  glomerular sections per group). All data are shown as mean  $\pm$  standard error of the mean. Statistical significance between each group is represented by a horizontal bar.

\* $P < 0.05$  by ANOVA with Tukey post hoc test.



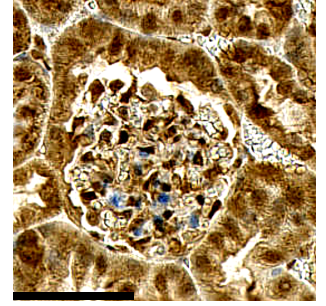
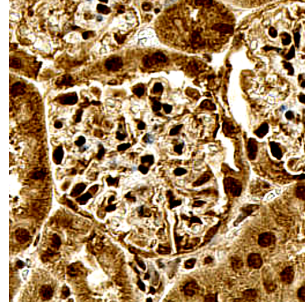
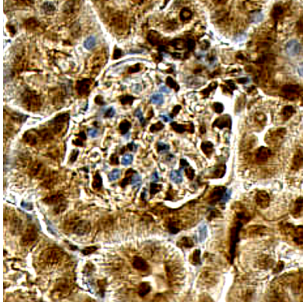
**A.**

db/m

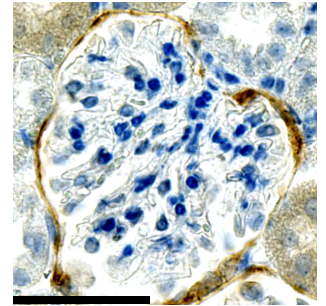
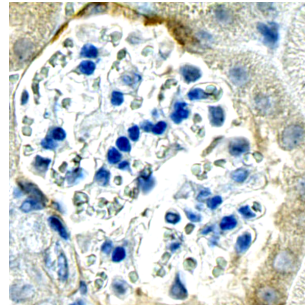
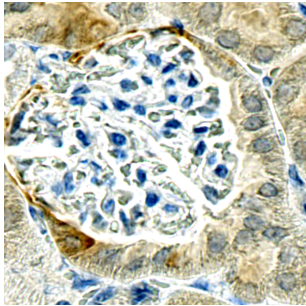
db/db

NMN500

Sirt1



Claudin-1



Synaptopodin

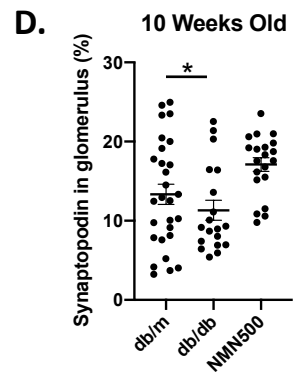
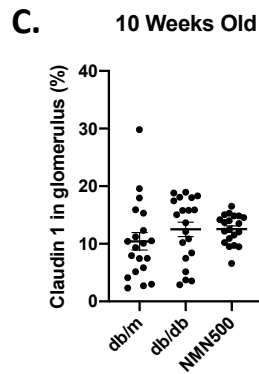
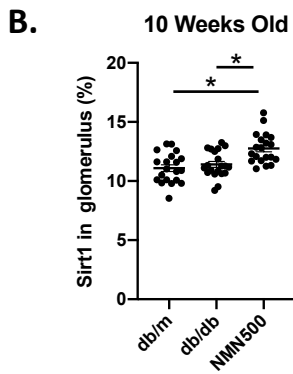
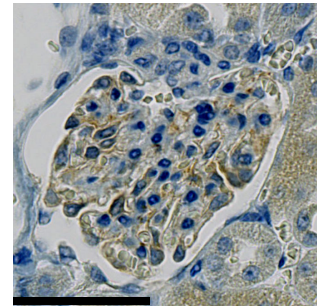
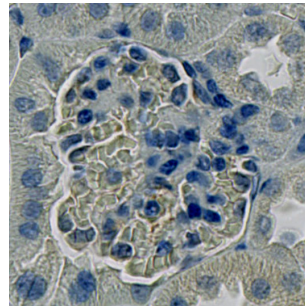
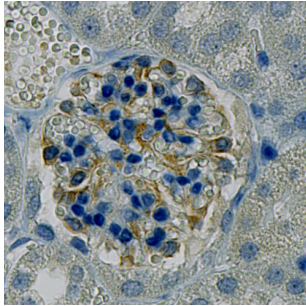


Figure S7, Yasuda *et al.*

**Figure S7. Molecular changes in glomerulus at 10 weeks of age**

(A) Representative immunostaining for Sirt1, Claudin-1, and Synaptopodin in the glomeruli of the *db/m*, *db/db*, and NMN500 groups at 10 weeks of age (scale bar, 50  $\mu$ m). (B–D)

Proportional areas of Sirt1 (B), Claudin-1 (C), and Synaptopodin (D) staining determined by Image-Pro Plus 7.0J software ( $n = 20$  glomerular sections per group). All data are shown as mean  $\pm$  standard error of the mean. Statistical significance between each group is represented by a horizontal bar. \* $P < 0.05$  by ANOVA with Tukey post hoc test.

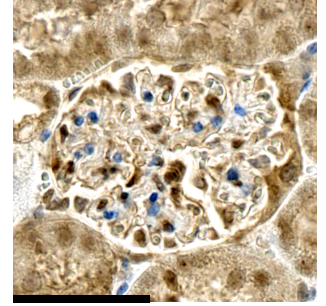
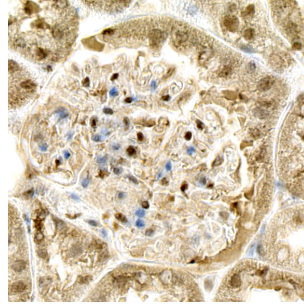
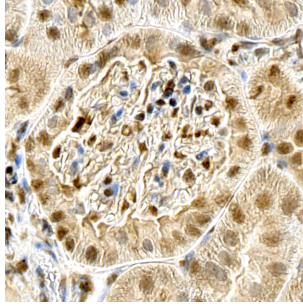
**A.**

db/m

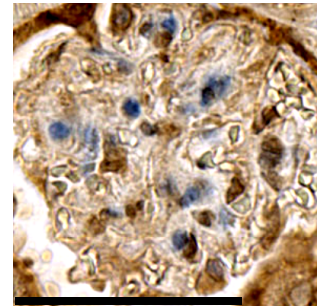
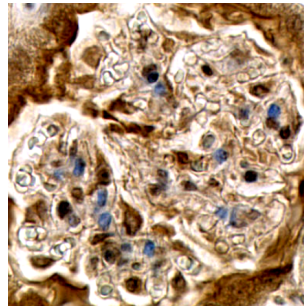
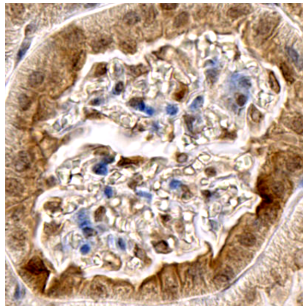
db/db

NMN500

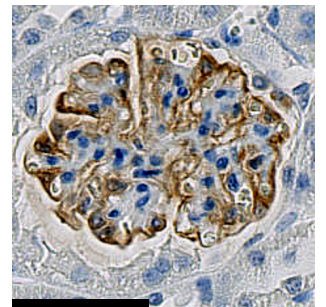
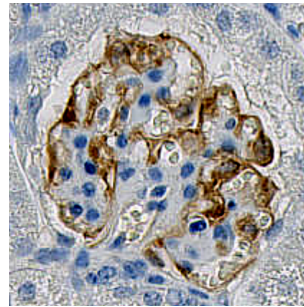
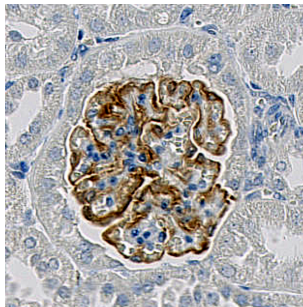
Sirt1



Claudin-1

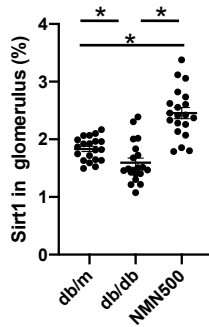


Synaptopodin



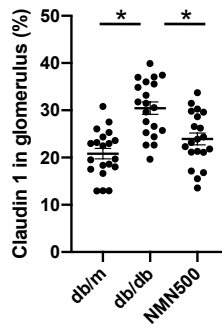
**B.**

30 Weeks Old



**C.**

30 Weeks Old



**D.**

30 Weeks Old

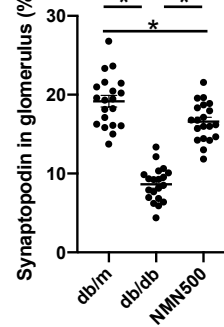


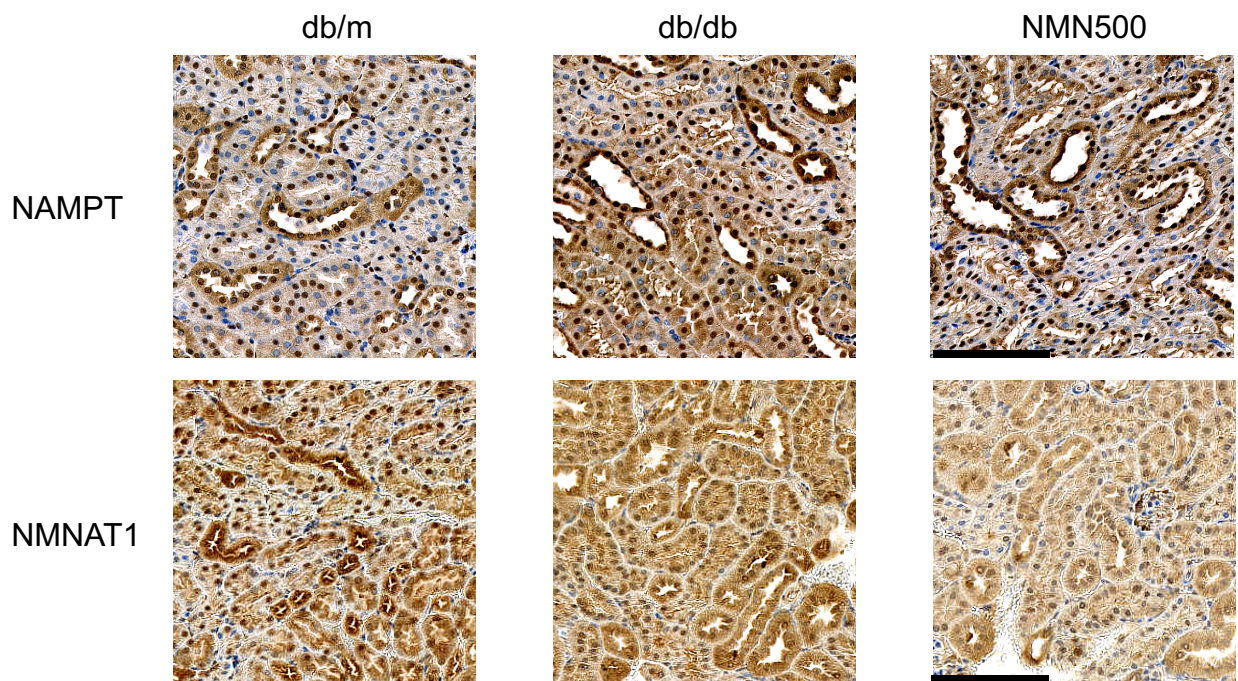
Figure S8, Yasuda *et al.*

**Figure S8. Molecular changes in glomerulus at 30 weeks of age**

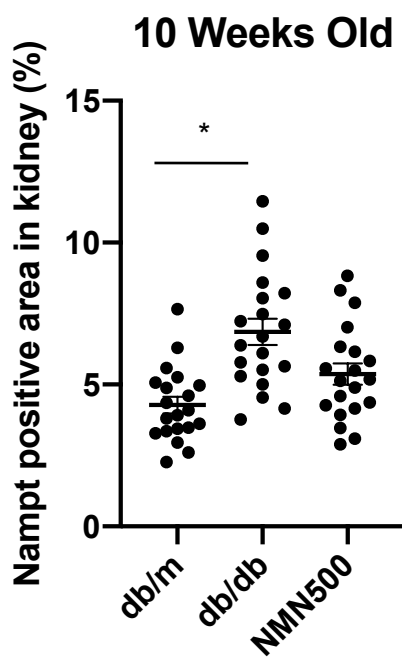
(A) Representative immunostaining for Sirt1, Claudin-1, and Synaptopodin in the glomeruli of the *db/m*, *db/db*, and NMN500 groups at 30 weeks of age (scale bar, 50  $\mu$ m). (B–D)

Proportional areas of Sirt1 (B), Claudin-1 (C), and Synaptopodin (D) staining determined by Image-Pro Plus 7.0J software ( $n = 20$  glomerular sections per group). All data are shown as mean  $\pm$  standard error of the mean. Statistical significance between each group is represented by a horizontal bar. \* $P < 0.05$  by ANOVA with Tukey post hoc test.

**A.**



**B.**



**C.**

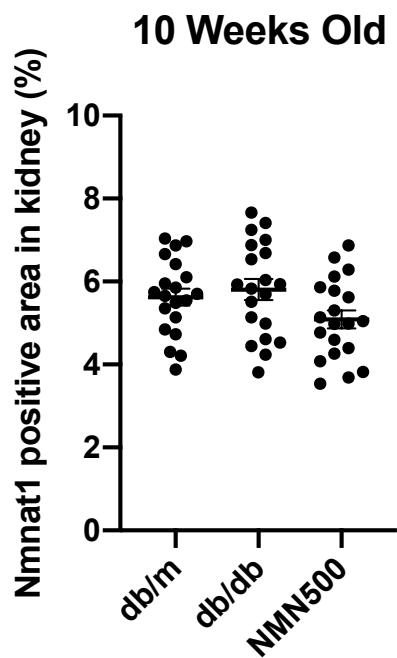
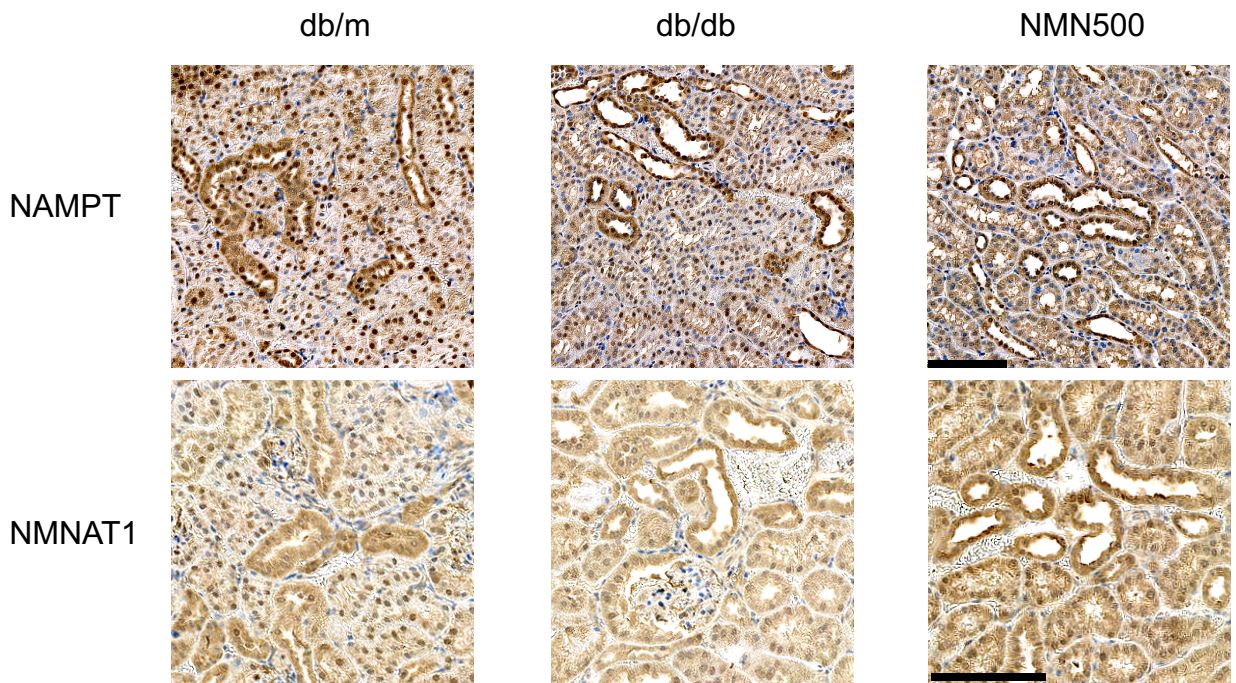


Figure S9, Yasuda *et al.*

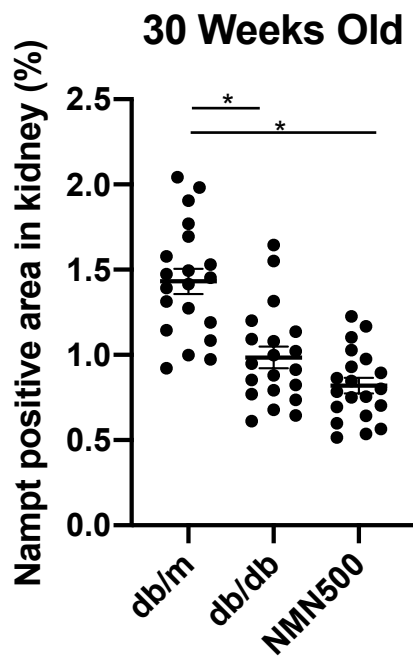
**Figure S9. Effects of NMN treatment on the salvage pathway at 10 weeks of age**

(A) Representative immunostaining for Nampt, Nmnat1 in the kidneys of the *db/m*, *db/db*, and NMN500 groups at 10 weeks of age (scale bar, 100  $\mu$ m). (B, C) Proportional staining areas for Nampt (B) and Nmnat1 (C) determined by Definiens Tissue Studio software ( $n = 20$  sections / group). All data are shown as mean  $\pm$  standard error of the mean. Statistical significance between each group is represented by a horizontal bar.  $*P < 0.05$  by ANOVA with Tukey post hoc test.

**A.**



**B.**



**C.**

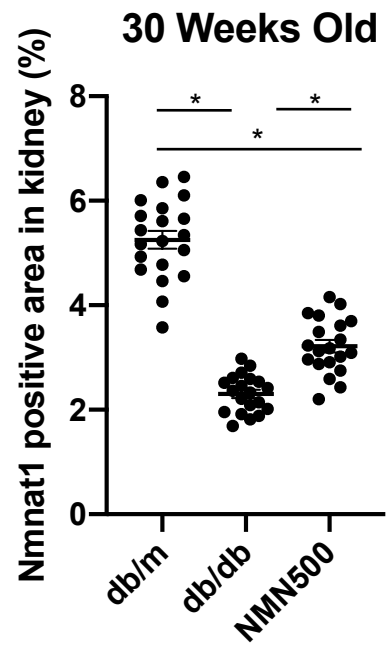


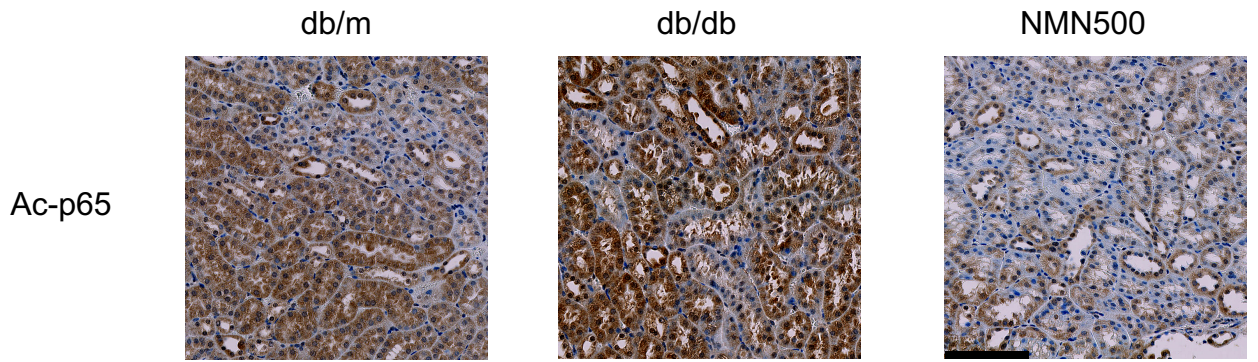
Figure S10, Yasuda *et al.*

**Figure S10. Effects of NMN treatment on the salvage pathway at 30 weeks of age**

(A) Representative immunostaining for Nampt, Nmnat1 in the kidneys of the *db/m*, *db/db*, and NMN500 groups at 30 weeks of age (scale bar, 100  $\mu$ m). (B, C) Proportional staining areas for Nampt (B) and Nmnat1 (C) determined by Definiens Tissue Studio software ( $n = 20$  sections/group). All data are shown as mean  $\pm$  standard error of the mean. Statistical significance between each group is represented by a horizontal bar.  $*P < 0.05$  by ANOVA with Tukey post hoc test.



**A.**



**B.**

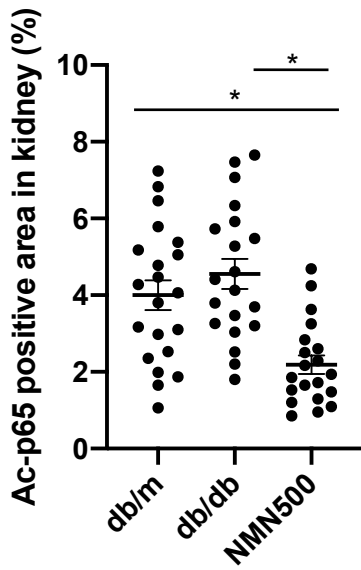


**Figure S11. Effect of NMN treatment on acetylated p65**

(A) Representative immunostaining for acetylated p65 (Ac-p65) in the kidneys of the *db/m*, *db/db*, and NMN500 groups at 24 weeks of age (scale bar, 100  $\mu$ m). (B) Proportional staining areas for Ac-p65 determined by Image-Pro Plus 7.0J software ( $n = 20$  sections / group). All data are shown as mean  $\pm$  standard error of the mean. Statistical significance between each group is represented by a horizontal bar.  $*P < 0.05$  by ANOVA with Tukey post hoc test.